

Butane Hydroisomerisation Using Pt-Promoted OSDA-Free Zeolite Beta

Ka Yan Cheung,^[a] Sam Schouterden,^[a] Sam Van Minnebruggen,^[a] Patrick Tomkins,^[a] Trees De Baerdemaeker,^[b] Andrei-Nicolae Parvulescu,^[b] Toshiyuki Yokoi,^[c] Dirk De Vos^{*[a]}

^a Centre for Membrane Separations, Adsorption, Catalysis and Spectroscopy for Sustainable Solutions (cMACS), Leuven Chem&Tech, KU Leuven, 3001 Leuven, Belgium

^b Process Research and Chemical Engineering, BASF SE, 67056 Ludwigshafen, Germany

^c Nanospace Catalysis Unit, Institute of Innovative Research, Tokyo Institute of Technology, 226-8503 Yokohama, Japan

*Corresponding author: dirk.devos@kuleuven.be

Abstract

Hydroisomerisation of *n*-butane to isobutane is a challenging reaction, even for Pt-loaded zeolites with strong acid sites. In comparison with 10-membered ring (10MR) zeolites, 12-membered ring (12MR) zeolites give consistently higher isomerisation yields. We report that besides the known catalysts with *BEA topology, also three-dimensional frameworks with MSE and YFI topologies (with Si/Al ~10) are suitable to obtain high isobutane selectivities and yields. As an alternative to Beta zeolites obtained *via* templated synthesis, Beta zeolites prepared *via* a template-free synthesis proved to be more active at lower temperatures and delivered higher isobutane yields in such conditions. Side reactions such as the Pt-catalysed hydrogenolysis were successfully suppressed by decreasing the Pt content, even in hydrogen rich conditions. Isobutane yields up to 31% were achieved in a single pass.

Introduction

Isobutane is in high demand as a reactant in the alkylation of butenes with isobutane, leading to high-octane C₈ compounds, or, after dehydrogenation to isobutene, as a reactant to make butyl rubber (isobutylene isoprene rubber), methyl *tert*-butyl ether, *tert*-butylamine *etc.*^[1,2] Isomerisation of linear butane to isobutane is therefore practised industrially, classically using a chlorinated alumina combined with Pt, as in the Butamer® process of UOP.^[3] Adding platinum helps to reduce coke formation. While the chlorine is essential for the isomerisation activity, the metal stimulates the loss of chlorine from the catalyst, causing the catalytic performance to deteriorate progressively. Also a reducing hydrogen atmosphere induces departure of the chlorine from the catalyst's surface.^[4] Other catalysts such as sulfated zirconia^[5] and alumina-promoted sulfated zirconia have been looked into by numerous groups; Wang *et al.* showed that on alumina-promoted sulfated zirconia, monomolecular isomerisation dominated, with a primary carbenium ion as a necessary intermediate. This explains the high selectivity to isobutane, albeit accompanied again by a rapid decline in catalytic activity.^[6]

To solve such challenges, acid zeolites have been investigated as alternative catalysts. Literature on zeolite-catalysed butane isomerisation focuses on a small number of privileged topologies, like MFI, MOR and *BEA. The dimensionality of the pore system can influence the mechanism that is operating. Thus, bimolecular encounters seem less likely in a monodimensional pore system like that of mordenite.^[7] On the other hand, in a zeolite with monodimensional pores, diffusion pathways can be longer, and primary reaction products may undergo many successive reactions during their diffusion out of the pore system. This would favour formation of compounds like propane. Besides the pore diameter, which is obviously larger for 12MR than for 10MR zeolites, also the availability of cages or spacious channel intersections, like in MFI or *BEA, can influence the intermediates that can be formed, and thus the eventual product distribution. Additionally, the framework Si/Al ratio plays a decisive role. For zeolites in which the Si/Al ratio has been raised by dealumination, it is assumed that the residual Brønsted acid sites are stronger, and at sufficiently high temperature, this can enable butane isomerisation by the monomolecular mechanism. Lower Si/Al ratios have been associated with higher densities of acid sites, and increased rates of reaction *via* bimolecular mechanisms.

In bifunctional zeolites, combining Pt or Pd metal nanoparticles with acid sites, there is a subtle interplay between both types of sites. By hydrogenating coke precursors, the metal circumvents the fast deactivation that is commonly observed with monofunctional, protonic zeolites. Even in the presence of H₂, the metal facilitates the dehydrogenation to butenes; higher butene pressures increase the likelihood of bimolecular reactions, which produce besides isobutane, also less desirable products like propane and pentane. Like in all bifunctional catalysts, it is desirable to reach a sufficient intimacy between the metallic and acid function; if *e.g.* isobutene needs to travel only a short distance before reaching a metallic site, this decreases the probability of secondary reactions and favours the isobutane yield. However, a too large number of available metal sites could also elicit reactions that only use the metal function, in particular hydrogenolytic cracking to undesired methane or ethane. In this sense, Cañizares proposed the ratio of strong acid sites to available metal sites as an important parameter governing the selectivity of the isomerisation

process.^[8,9] This concept also implies that the metal content and dispersion need to be adjusted to the acid site density and other characteristics of the zeolite material.

In this paper, we explore in detail the potential of *BEA topology zeolites for the butane isomerisation. Since the butane-isobutane equilibrium favours the branched isomer at lower temperature, we particularly focus on catalysts that give superior isobutane selectivity at moderate temperatures, and at medium to high conversion, in order to maximise the isobutane yield per pass, while limiting the formation of less desired hydrocarbons like propane or pentanes. We first compare *BEA zeolites with zeolites with other topologies; this identifies *BEA zeolites as superior catalysts, but also reveals some zeolites with new topologies that could be interesting as butane isomerisation catalysts. The Beta zeolites reported so far all had Si/Al ratios of ~11 or more, as resulting from a typical hydrothermal synthesis in the presence of a template, potentially followed by dealumination. Beta zeolites with higher Al contents recently became accessible, *i.a. via* template-free synthesis.^[10] We hypothesised that the large number of strong acid sites in these zeolites could result in higher isobutane yields at lower temperatures. Therefore, this paper focuses on bifunctional catalysts for butane isomerisation prepared starting from Al-rich Beta zeolites.

Results and discussion

Selection of zeolite materials

Initial experiments were performed with H-zeolites, in the absence of a metal, but under hydrogen atmosphere, at 360°C. At these relatively low temperatures, *n*-butane conversion was small for the ZSM-5 sample (Si/Al = 25; Table 1, entry 1). Increased conversions were obtained with the 12MR Beta zeolites, and the conversion was higher for the Beta zeolite with Si/Al = 4.6 than with the material with Si/Al = 12.5 (Table 1, entries 2 and 3). The latter is prepared ('Beta-12.5') *via* a templated synthesis, and is similar to the Beta zeolites used in previous studies with metal-free H-zeolites;^[11] the former, with its unusually high Al content, results from an organotemplate-free synthesis ('OF-Beta-4.6'). In previous studies using this OF-Beta in reactions like the isobutane alkylation with butene, we showed that OF-Beta possesses large amounts of strong Brønsted acid sites.^[12,13] Regarding the product selectivity, the ZSM-5 sample displayed significantly lower selectivity for isobutane than both Beta zeolites (Table 1, entries 1-3); this finding is in agreement with the work of Zhang *et al.*, who observed as well isobutane selectivities below 20% for ZSM-5 in the absence of a noble metal. Conversely, for Beta-12.5 and OF-Beta-4.6, isobutane selectivities in a range between 50 and 60% were obtained, in good agreement with earlier observations;^[11,14] C₃ and C₅ compounds were the other dominant products.

Such a product distribution is largely consistent with a bimolecular mechanism, in which product formation proceeds through C₈ intermediates; if a monomolecular mechanism were dominant, much higher isobutane selectivities could be expected.^[11] For monofunctional zeolites, possessing only acid sites, butane must initially be activated by protonation to a butyl carbonium ion, followed by H₂ loss and formation of a butyl carbenium ion. In the proposal by Asuquo *et al.*,^[15] the latter could alkylate another butane molecule to form a C₈ carbonium ion; or the butyl carbenium ion could react in a dimerisation with a butene to form a C₈ carbenium ion. Rearrangement and cracking of the octyl carbenium eventually, after hydrogen transfer, can yield butane and isobutane, resulting in a net C₄ isomerisation; on the other hand, cracking of the C₈ carbenium and C₈ carbonium ions could also produce C₃ and C₅ products. For acid mordenites, Asuquo has proposed that higher acid site densities favour formation of C₃ and C₅ products *via* octyl carbonium intermediates.^[15] A decrease of the *i*-C₄ selectivity (from 59 to 51%) is seen for the Beta zeolites upon decreasing the Si/Al ratio from 12.5 to 4.6 (Table 1, entries 2-3); but the effect is relatively weak, and the changed selectivity may as well partly be due to the higher conversion with the OF-Beta material.

The beneficial effects of noble metals like Pt or Pd on the isomerisation of alkanes are well known. On the metal sites, butane can be dehydrogenated to form butenes, even with H₂ in the background, resulting in C₄ carbenium ion formation on the Brønsted acid sites. It has been proposed that one metal site could already provide for hundreds of acid sites;^[16] so a small amount of Pt already triggers the bifunctionality.^[17-20] Bifunctional zeolites have been tested in the literature for butane isomerisation in widely diverging reaction conditions, *e.g.* regarding temperature, WHSV, H₂:butane ratio; therefore a range of metal-loaded zeolites with a low 0.5wt% Pt loading were tested here in identical conditions, with a focus on identifying the materials that give the highest isobutane yields, as well as the best selectivities for isobutane. As is seen in Table 1, with the

addition of platinum, the butane conversion improved drastically (entries 4-10). With none of the samples based on 10MR zeolites, high *i*-C₄ selectivities were observed (entries 4-6). At 25% conversion, similar *i*-C₄ selectivities were obtained with MCM-22 and ZSM-5 (18-19%; entries 5-6). The high C₁+C₂ selectivity seen with ferrierite, ZSM-5, and MCM-22 indicates that even 0.5wt% Pt induces too much hydrogenolytic cracking,^[18,19,21-24] and the large selectivity for C₃+C₅ products suggests that secondary cracking may occur before the primary products can leave the 10MR zeolite pores. Overall, in the conditions considered, higher *i*-C₄ yields were realised with the 12MR zeolites (entries 7-10); with these catalysts, the isomerisation is generally favoured over hydrogenolytic cracking to products like C₁ and C₂. With all 12MR zeolites tested, the *i*-C₄ selectivity at 25% conversion exceeds the C₃+C₅ selectivity. A possible reason has been postulated by Zhang and Adeeva (Scheme 2); the higher isobutane selectivity could be traced back to the larger space in the zeolite structures, allowing the formation of the bulkier trimethylpentane C₈ cations (*vs* dimethylhexane C₈ cations) which then give isobutane.^[14,25] This route is less favoured in the smaller voids of 10MR zeolites.

In comparison with the other 12MR zeolites tested, USY reached only a small *i*-C₄ yield at 360 °C (Table 1, entry 7), in agreement with De Rossi *et al.* who found that USY was less active than H-mordenite.^[24] Therefore USY was not considered further. Despite showing the lowest hydrogenolysis activity in Table 1 (entry 8), mordenite is prone to fast deactivation (Figure S10), which has been ascribed by several groups to coke formation blocking the pores.^[15,18,26-28] Indeed, the unidirectional pore system of the MOR topology is highly susceptible to obstruction of the channels, making large portions of the active sites unavailable for catalysis.^[29,30] Mordenite also lacks spacious channels intersections, which makes it more difficult to form bulky intermediates. Since better isobutane yields and selectivities were achieved with *BEA materials, mordenite was not taken further in this study. At 0.5wt% Pt loading, the Beta zeolites combine good *i*-C₄ yields with *i*-C₄ selectivities up to 65% at 25% conversion. As with the Pt-free catalysts, the *i*-C₄ production increases as the Al-content of the material is increased (Table 1, entry 10 *vs* 9).

Table 1. Activity at 360 °C of selected zeolites, either metal-free or loaded with 0.5wt% Pt *via* ion exchange. Selectivity values reported at 25% butane conversion.

Entry	Catalyst	Si/Al	<i>X</i> ^a (%)	<i>Y</i> ^b (%)	<i>S</i> ^c (%)			<i>T</i> ^d °C
					<i>i</i> -C ₄	C ₁ +C ₂	C ₃ +C ₅	
1	ZSM-5 ^e	25	1.4	0.1	11 ^f	26 ^f	63 ^f	360
2	Beta-12.5 ^e	12.5	3.6	2.1	59 ^f	7 ^f	34 ^f	360
3	OF-Beta-4.6 ^e	4.6	13.4	6.8	51 ^f	3 ^f	44 ^f	360
4	Ferrierite	6.15	16.8	1.1	7	55	38	374
5	ZSM-5	25	77.5	13.2	19	44	36	320
6	MCM-22	16.7	99.8	0.6	18	52	30	304
7	USY	15	12.2	4.7	39 ^f	32 ^f	28 ^f	360
8	Mordenite	6.75	41.3	16.8	56	4	39	326
9	Beta-12.5	12.5	33.0	19.1	56	18	24	339
10	OF-Beta-4.6	4.6	39.7	24.5	65	11	23	333

Reaction conditions: P_{butane} 0.15 bar, P_{hydrogen} 0.85 bar, WHSV 3.5 h⁻¹.

^a Butane conversion.

^b Isobutane yield.

^c Selectivity at 25% butane conversion.

^d Temperature at which the selectivities are reported.

^e Zeolite with no added metal content.

^f Selectivity of samples that could not reach 25% butane conversion.

Table 2. Activity at 360 °C of selected zeolites loaded with 0.1wt% Pt *via* ion exchange. Selectivity values reported at 25% butane conversion.

Entry	Catalyst	Si/Al	X^a (%)	Y^b (%)	S^c (%)			T^d °C
					<i>i</i> -C ₄	C ₁ +C ₂	C ₃ +C ₅	
1	Ferrierite	6.15	12.9	3.1	25	40	35	382
2	ZSM-5	25	43.4	18.3	41	28	31	338
3	MCM-22	16.7	54.7	21.4	45	32	23	330
4	Beta-12.5	12.5	38.6	22.9	62	13	24	342
5	OF-Beta-4.6	4.6	35.0	24.4	76	2	21	345
6	MCM-68	10	33.7	20.8	65	10	24	347
7	YNU-5	9.8	42.3	19.8	54	13	32	335

Reaction conditions: P_{butane} 0.15 bar, P_{hydrogen} 0.85 bar, WHSV 3.5 h⁻¹.

^a Butane conversion.

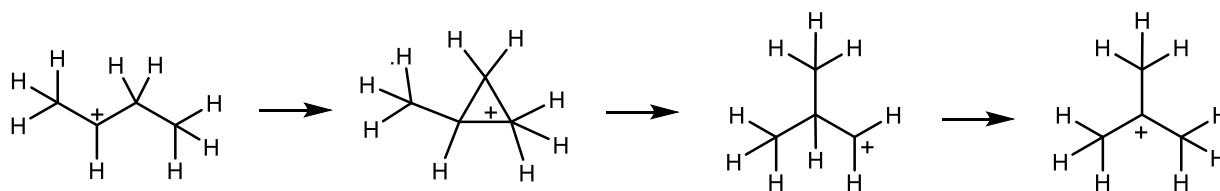
^b Isobutane yield.

^c Selectivity at 25% butane conversion.

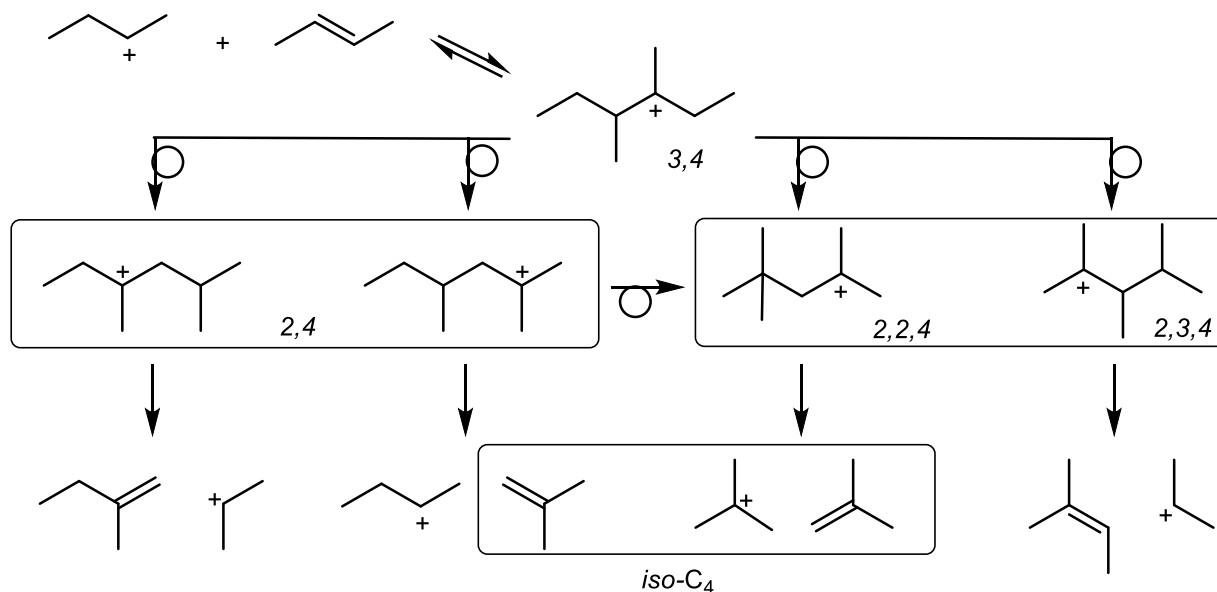
^d Temperature at which the selectivities are reported.

As in particular for 10MR zeolites high hydrogenolysis activity was recorded (Table 1, entries 4-6), catalytic activity of Pt loaded zeolites was also measured at 0.1wt% Pt (Table 2). As expected, selectivity towards the hydrogenolysis products C₁ and C₂ fell, since a reduced metal content results in fewer metal sites.^[17] This was coupled to a sharp improvement in the *i*-C₄ selectivity across the board, not only for the 10MR zeolites ZSM-5 and MCM-22 (entries 2-3), but also for the 12MR Beta zeolites (entries 4-5). The balance between metal and acid sites is now more favourable to the desired isomerisation, especially on the Al-rich OF-Beta-4.6: the C₁+C₂ selectivity ($X = 25\%$) decreases to 2%, while the *i*-C₄ selectivity reaches 76%, which is substantially higher than is observed on the best, well-studied mordenite catalysts (selectivity for *i*-C₄ $\cong 55\%$ at 5-20% conversion).^[17] Even higher *i*-C₄ selectivities, up to 90% at 21% conversion, have been observed for other catalyst types like sulfated ZrO₂, although it is known that this *i*-C₄ selectivity decreases with temperature.^[11] In the case of sulfated ZrO₂, the preferred formation of *i*-C₄ has been interpreted as arising from a monomolecular mechanism, which is energetically quite demanding since it requires a protonated cyclopropane ring to be opened to form a primary carbenium ion (Scheme 1).^[31] However, for the Beta catalysts, the high *i*-C₄ selectivities do not necessarily imply that there is an increased contribution of the monomolecular mechanism. In the vision of Adeeva,^[25] the dimethylhexyl carbenium ions, which are initially formed in the bimolecular mechanism, can isomerise to trimethylpentyl carbenium ions. These are identical to the intermediate carbocations formed in the alkylation of isobutane with butenes.^[32] Specifically

in the case of isobutane alkylation with Beta zeolites, including the OF-Beta,^[13,32,33] it is known that the reaction produces 2,2,4-trimethylpentane as the dominant C₈ isomer. This indicates that C₈ carbenium ion isomerisation in Beta zeolites favours formation of the 2,2,4-trimethylpentyl tertiary carbenium ion (Scheme 2), which in the alkylation reaction serves as a direct precursor to 2,2,4-trimethylpentane. In the bimolecular butane isomerisation, the product selectivity depends on the nature and scission rates of the C₈ carbenium ions. It should be remarked that β-scission of the 2,2,4-trimethylpentyl carbenium ion is kinetically very strongly favoured, since besides the olefin (isobutene), a new tertiary carbenium is formed.^[34] Remarkably, the β-scission of the 2,2,4-trimethylpentyl cation produces two fragments with an iso-C₄ skeleton. Summarising, the well-documented preference of Beta zeolites to form 2,2,4-trimethylpentane skeletons can contribute to increased isobutane selectivity in the butane isomerisation.



Scheme 1. Skeletal isomerisation of a linear butyl carbenium ion to a branched butyl carbenium ion *via* a monomolecular mechanism implies formation of a primary carbenium ion.



Scheme 2. Formation, isomerisation and β-splitting of carbenium ions involved in bimolecular butane isomerisation.^[14]

Additionally, two materials that were not tested so far in butane isomerisation have been included here, *viz.* MCM-68 and YNU-5 (Table 2, entries 6 and 7); like Beta zeolites, they are both three-dimensional materials with at least one 12-membered ring, with MSE and YFI topology respectively.^[35,36] At comparable Si/Al ratios, they generated similar conversions and isobutane yields as Beta-12.5 at 360 °C, as well as similar isobutane selectivities (54-65%) at 25% butane conversion. MCM-68 (Si/Al = 10) and YNU-5 (Si/Al = 9.8) have a similar NH₃-TPD profile and number of strong acid sites as Beta-12.5 (compare Figure S7 with Figure 4).

Role of Pt loading and method of Pt introduction

To highlight the impact of Pt loading on the hydrogenolysis activity and the isobutane selectivity, a series of different platinum contents was tested, first using the templated zeolite Beta with Si/Al = 12.5. The strong acid sites in this material were quantified based on NH₃-TPD, by integration of the high temperature desorption peak (Table S3). Initially, Pt was introduced *via* ion exchange. Table 3 reports the catalytic performance, the Pt dispersion and the number of available Pt sites as measured by CO chemisorption, and the ratio of strong acid sites to available metal sites ($n_{\text{acid}}/n_{\text{Pt}}$). The experimental results for 0.1wt% Pt and 0.5wt% Pt prepared by ion exchange were close; both samples give a similar *i*-C₄ selectivity (57-59 %), with 0.5wt% Pt giving an only slightly higher C₁+C₂ selectivity. Table 3 suggests a relation between high *i*-C₄ selectivity, and a large number of acid sites per number of available Pt sites ($n_{\text{acid}}/n_{\text{Pt}} \geq 50$). As the Pt content is increased, *e.g.* to between 2 and 5%, there is a sharp drop in the *i*-C₄ selectivity, while the selectivities for the hydrogenolysis products C₁ and C₂, and for propane increase (Figure 1). Parallely, the $n_{\text{acid}}/n_{\text{Pt}}$ ratio decreases to 15 or less. This is readily interpreted based on literature insights: when the metal content is too high, secondary reactions that are catalysed by metal particles, in particular hydrogenolytic cracking to methane and ethane, become increasingly dominant in the product distribution.^[9] Propane as well is a potential product of direct butane hydrogenolysis.^[21] Moreover, if the dehydrogenation activity is increased, olefins become more abundant,^[37] comprising not only butenes, but also pentenes. Consequently, C₉ intermediates are readily formed, *e.g.* by reaction of butyl carbenium ions with pentenes, and these C₉ species are easily cracked to form significant amounts of propane.^[17]

Table 3. Characteristics of Pt-loaded Beta-12.5 and performance in butane isomerisation.

Entry	Pt content (wt%)	X ^a (%)	S ^b (%)				Pt dispersion ^c (%)	Monolayer CO uptake ^c (μmol/g _{sample})	$n_{\text{acid}}/n_{\text{Pt}}$ ^d
			<i>i</i> -C ₄	C ₁ +C ₂	C ₃	C ₅			
1	0	4	59	7	23	11	NA	NA	NA
2	0.1	39	59	10	20	9	31	1.6	406
3	0.5	33	57	16	19	5	48	12.4	52
4	2.0	63	24	41	33	1	57	60.7	11
5	2.0 ^e	46	51	18	24	5	37	38.9	17
6	3.5	78	15	48	35	0	64	117.0	6
7	5.0	92	8	55	36	0	66	174.1	4

Reaction conditions: P_{butane} 0.15 bar, P_{hydrogen} 0.85 bar, WHSV 3.5 h⁻¹, 360 °C.

^a Butane conversion.

^b Selectivity values.

^c Obtained from CO chemisorption.

^d The number of strong acid sites was obtained by deconvolution of the NH₃-TPD profiles; for Beta-12.5, $n_{\text{acid}} = 0.65 \text{ mmol g}^{-1}$.

^e Pt loaded using incipient wetness impregnation, ion exchange in all other cases.

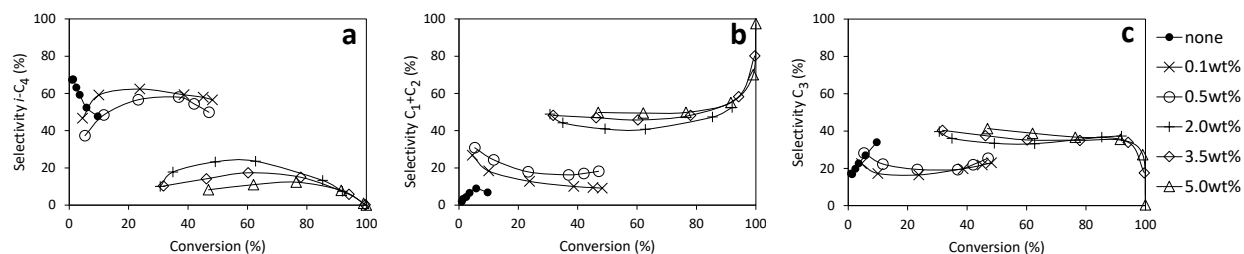


Figure 1. Selectivity-conversion plots of *i*-C₄ (a), C₁+C₂ (b), C₃ (c) using templated Beta-12.5 with various Pt contents loaded by ion exchange. $P_{\text{butane}} 0.15 \text{ bar}$, $P_{\text{hydrogen}} 0.85 \text{ bar}$, $\text{WHSV } 3.5 \text{ h}^{-1}$, varied temperature.

Besides the metal content, also the metal incorporation technique can affect the dispersion of the metal, and thus the number of available Pt sites. Aqueous ion exchange (IEX) and incipient wetness impregnation (IWI) were used to incorporate 0.5wt% and 2wt% Pt on the templated Beta. For catalysts with 0.5wt% Pt, differences were minor (Figure 2), with similar catalytic performance regardless of the metal incorporation method. At the higher loading of 2wt% Pt, there was a stark contrast in the results (Figure 3): for the ion-exchanged sample, the butane conversion was notably higher but isobutane selectivity was particularly low. As the data show, the sample prepared by IWI has a poorer metal dispersion and hence, a lower number of available Pt sites and a higher $n_{\text{acid}}/n_{\text{Pt}}$ ratio (Table 3, entries 4 and 5). As the data show, a sufficiently high $n_{\text{acid}}/n_{\text{Pt}}$ ratio is important to maintain high *i*-C₄ selectivity. Summarising, for a zeolite with a given number of acid sites, it is important to keep the number of available Pt sites sufficiently low, either by limiting the dispersion, or more favourably, by limiting the Pt content.

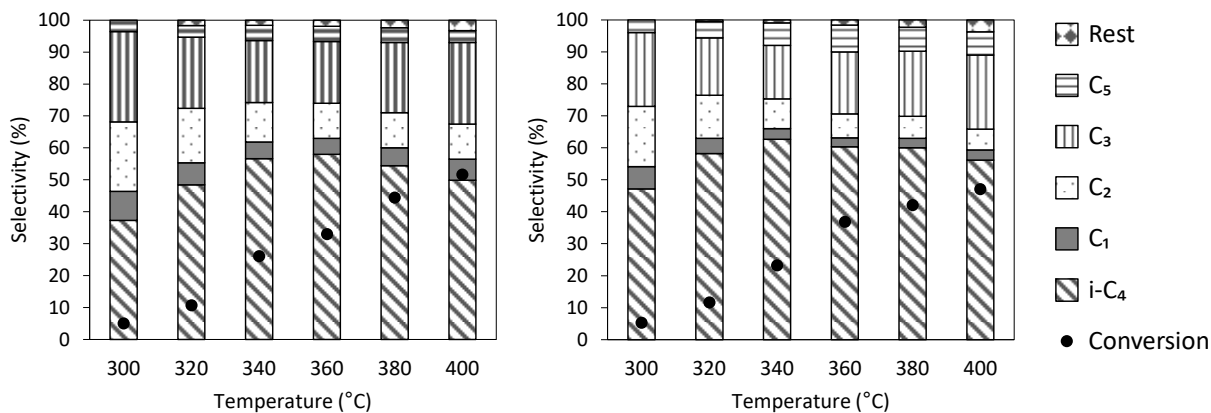


Figure 2. Conversion and product distribution of *n*-butane isomerisation using 0.5wt% Pt/Beta-12.5. Pt was incorporated by ion exchange (left) or impregnation (right). $P_{\text{butane}} 0.15 \text{ bar}$, $P_{\text{hydrogen}} 0.85 \text{ bar}$, $\text{WHSV } 3.5 \text{ h}^{-1}$, varied temperature.

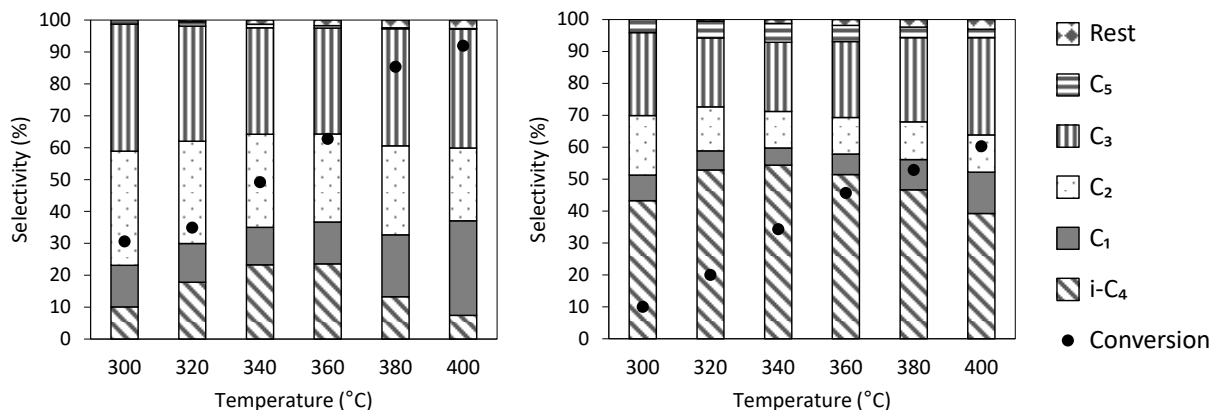


Figure 3. Conversion and product distribution of *n*-butane isomerisation using 2wt% Pt/Beta-12.5. Pt was incorporated by ion exchange (left) or impregnation (right). P_{butane} 0.15 bar, P_{hydrogen} 0.85 bar, WHSV 3.5 h^{-1} , varied temperature.

Table 4. Textural properties of selected samples.

Sample	Si/Al	Surface area (m^2/g)			$V_{\text{micro}}^{\text{c}}$ (cm^3/g)	$V_{\text{meso}}^{\text{d}}$ (cm^3/g)
		$S_{\text{BET}}^{\text{b}}$	$S_{\text{micro}}^{\text{c}}$	$S_{\text{EXT}}^{\text{c}}$		
Beta-12.5	12.5	582	376	206	0.165	0.207
Beta-9	9	646	398	248	0.180	0.213
Beta-5.2	5.2	616	481	135	0.197	0.107
OF-Beta-4.6	4.6	584	497	87	0.198	0.034
0.1-OF-Beta-4.6 ^a	4.6	421	349	72	0.139	0.028
0.5-OF-Beta-4.6 ^a	4.6	399	336	63	0.134	0.024

^a OF-Beta with Pt loaded *via* ion exchange; amount of Pt loading denoted at the front.

^b BET p/p_0 range = 0.00001 – 0.01.

^c Micropore area, external area, and micropore volume estimated from t-plot method.

^d Mesopore volume estimated by DFT method.

Performance of OSDA-free Beta zeolite in C_4 isomerisation

Despite extensive literature attention for (metal-loaded) *BEA zeolites as butane isomerisation catalysts, so far only Beta zeolites with Si/Al ratios of 11 or higher have been studied.^[9,11,18,20,22,38,39] Strikingly, better performance, *e.g.* higher *i*- C_4 selectivity is consistently obtained as the Si/Al ratio is decreased. Invariably, these Beta zeolites were obtained by a templated synthesis. In recent years, attention has been devoted to the synthesis of Beta zeolites that are prepared in the absence of OSDAs (organic structure directing agents). These OSDA-free Beta are prepared *i.a. via* seeded syntheses,^[10] and have a much lower Si/Al ratio.^[40] Production of OSDA-free Beta can be more advantageous as the process generates less emissions by avoiding the combustion for the template removal.^[12] Against this background, the performance of the templated Beta (Si/Al = 12.5) was

compared in detail with that of an OSDA-free Beta (Si/Al = 4.6). As proven by the NH₃ temperature programmed desorption results (Figure 4), the OSDA-free Beta possesses a high density of strong acid sites, *viz.* 1.43 mmol g⁻¹ for OF-Beta-4.6, *vs* 0.65 mmol g⁻¹ for Beta-12.5. The textural properties of these Beta materials are shown in Table 4, Figure S4 and Figure S5.

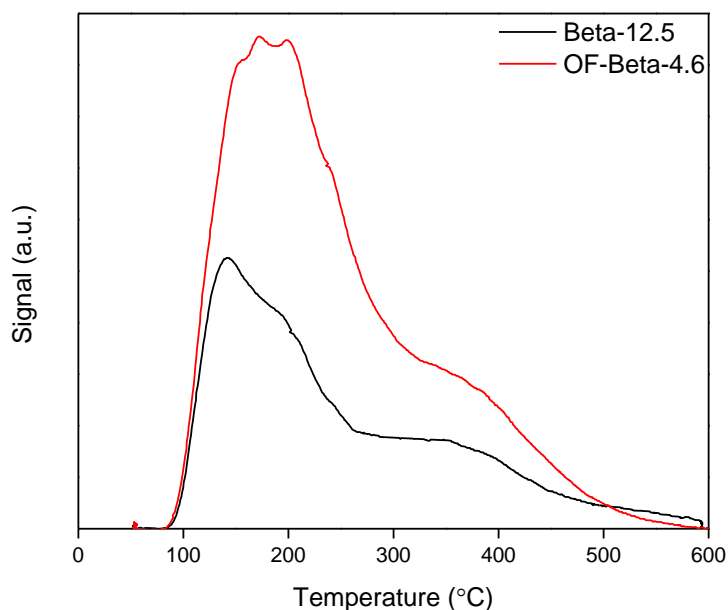


Figure 4. NH₃-TPD profiles of Beta-12.5 and OF-Beta-4.6. The number after the hyphen indicates the Si/Al ratio.

Comparing the templated Beta with the OSDA-free Beta at a Pt-loading of 0.5wt% (Table 5, entries 1 *vs* 2), the OSDA-free Beta reached higher conversion and *i*-C₄ yield at the same temperature of 360 °C. At an equal conversion of 45%, the *i*-C₄ selectivity was higher for the OSDA-free Beta, which was primarily due to a better suppression of hydrogenolysis. The Pt dispersion is similar in both catalysts at an identical loading of 0.5wt% Pt; however, the balance between the metal function and the amount of acid sites is clearly better in the OSDA-free OF-Beta-4.6 than in the templated Beta-12.5 with its smaller amount of acid sites. For the OF-Beta-4.6, the $n_{\text{acid}}/n_{\text{Pt}}$ ratio was almost twice that of the templated Beta-12.5 (Table 6).

A breakdown of the products is given in Figure 5 for both Beta samples with 0.5wt% Pt. The relatively high C₁-C₃ selectivity values at low conversions are due to hydrogenolysis being dominant at low temperatures (Figure 5a, b). From 320 °C on, *i*-C₄ selectivities reach higher values, in particular for OSDA-free Beta. As discussed before, this can still be compatible with a bimolecular pathway, since this mechanism has a lower energy of activation than the monomolecular mechanism in which primary carbenium ions need to serve as intermediates.^[15]

While formation of carbenium ions requires only one proton at a time, the high density of acid sites can still privilege the bimolecular mechanism, since a butene could be physisorbed on a Brønsted acid site in close vicinity of an already formed butyl carbenium ion, thus facilitating the formation of octyl carbenium ions in the bimolecular mechanism.^[14] As expected, the C₅ selectivity decreases while the C₃ selectivity increases with rising temperature and conversion, with the formation of C₉ intermediates as a logical contributing pathway.^[17,41]

Table 5. Activity of 0.5wt% Pt-loaded templated Beta-12.5 ('Beta'), and OSDA-free Beta-4.6 ('OF-Beta').

Catalyst	Si/Al	X ^a (%)	Y ^b (%)	S ^c <i>i</i> -C ₄ (%)	S ^c C ₁ +C ₂ (%)	T ^d (°C)
		at 360 °C	at 360 °C	at 45% X ^a	at 45% X ^a	
Beta	12.5	33.0	19.1	54	17	382
OF-Beta	4.6	39.7	24.5	59	10	375

Reaction conditions: P_{butane} 0.15 bar, P_{hydrogen} 0.85 bar, WHSV 3.5 h⁻¹.

^a Butane conversion.

^b Isobutane yield.

^c Selectivity.

^d Temperature at which the selectivities are reported.

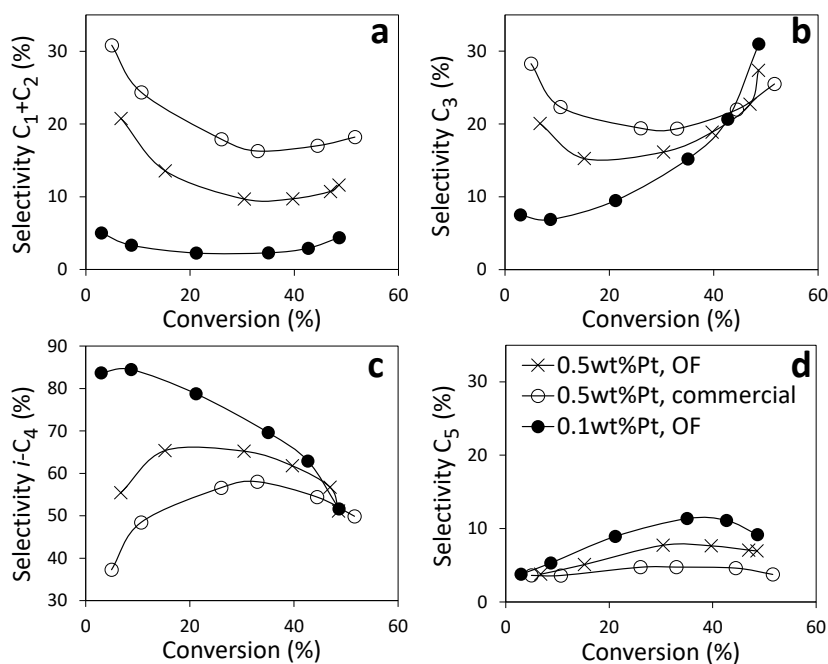


Figure 5. Selectivity-conversion plots of C₁+C₂ (a), C₃ (b), *i*-C₄ (c), and C₅ (d) using OF-Beta-4.6 and Beta-12.5, Pt loaded by ion exchange. P_{butane} 0.15 bar, P_{hydrogen} 0.85 bar, WHSV 3.5 h⁻¹, varied temperature.

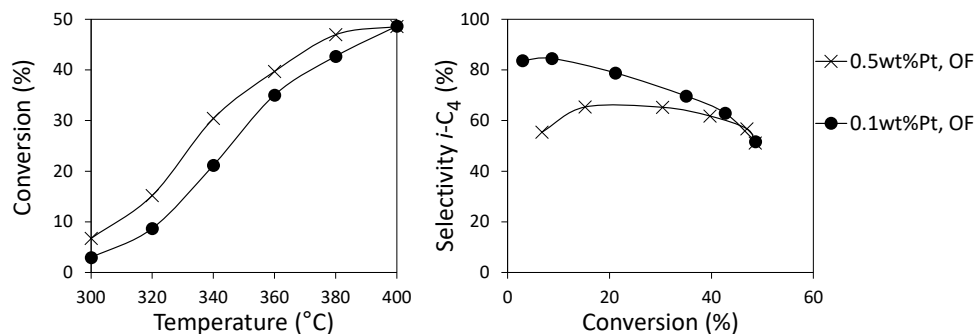


Figure 6. Conversion (left) and *i*-C₄ selectivity (right) obtained with OF-Beta-4.6, Pt loaded by ion exchange. P_{butane} 0.15 bar, P_{hydrogen} 0.85 bar, WHSV 3.5 h⁻¹.

Table 6. Characteristics of selected ion-exchanged Pt/Beta-12.5 and Pt/OF-Beta-4.6.

Catalyst	Pt content (wt%)	Dispersion ^a (%)	Monolayer CO uptake ^a (μmol/g _{sample})	$n_{\text{acid}}/n_{\text{Pt}}$ ^b
Beta-12.5	0.1	31	1.6	406
	0.5	48	12.4	52
OF-Beta-4.6	0.1	57	1.9	753
	0.5	55	14.1	101

^a Obtained from CO chemisorption.

^b Number of strong acid sites determined from NH₃-TPD.

Attempts to further improve the performance of OSDA-free Beta started with reducing the amount of platinum in the catalyst to 0.1wt%. Catalytic data are shown in Figure 5 and Figure 6; physical catalyst characteristics are presented in Table 6. While the conversion on OSDA-free Beta is slightly lower using 0.1 rather than 0.5wt% Pt, the hydrogenolysis activity is now successfully suppressed, even at low temperatures. This is easily rationalised based on the lower amount of accessible Pt sites and the resulting high $n_{\text{acid}}/n_{\text{Pt}}$ ratio of 753 for OSDA-free Beta with 0.1wt% Pt (Table 6). At conversions ≤ 21 %, the isobutane selectivity reaches values in the 78-84% range; meanwhile nearly equal amounts of C₃ and C₅ are formed. This proves that in these conditions, there are hardly secondary reactions, with loss of isobutane and formation of additional propane. Regarding the high *i*-C₄ selectivity, this could tentatively be ascribed to a contribution by a monomolecular mechanism; however also a bimolecular mechanism can generate large amounts of isobutane. As highlighted in Scheme 2, different carbenium ions like dimethylhexyl and trimethylpentyl ions can produce C₄, *iso*-C₄, C₃ and (*iso*)-C₅ compounds to different extents; thus the isomerisation rates and relative stabilities of the octyl carbenium ions in zeolites with varying structures will have a unique influence on the products formed.

Also the reaction parameters can be adapted to enhance isobutane formation. If the partial pressure of hydrogen is increased, the equilibrium of the dehydrogenation is shifted towards butane; the decreased olefin partial pressure generally disfavours bimolecular reactions; thus, it could limit secondary reactions, *e.g.* forming propane, and suppressing coke formation. More hydrogen can

improve catalyst stability by a ‘spillover effect’, in which the hydrogen molecules dissociate into atoms on the metal sites which can spill over to the acid sites to remove coke precursors which are unsaturated hydrocarbon species.^[42] However, increasing the $H_2/n-C_4$ ratio could also increase the hydrogenolysis rate.^[17] The data in Figure 7 show that this strategy is indeed successful for the OSDA-free Beta loaded with 0.1wt% Pt. As the $H_2/n-C_4$ ratio is increased from 85/15 to 95/5 or 97.5/2.5, the high *i*-C₄ selectivity is maintained over a wider range of conversion values (Figure 7b). The main side reaction seems to be hydrogenolysis, with methane being formed with clearly higher selectivity than in less hydrogen-rich conditions. The drop in C₃ formation at high conversion (Figure 7d) implies that higher $P(H_2)$ suppresses the bimolecular C₄ + C₅ reaction. Intriguingly, also C₅ formation is suppressed, even at low conversion (Figure 7e). Note that C₅ formation is a clear indicator for the bimolecular mechanism. This suggests that under these conditions of low partial pressure of butane, the isomerisation may to a significant extent proceed *via* a monomolecular mechanism on the strong acid sites of the OSDA-free Beta zeolite. Figure 7 also compares the behaviour of the OSDA-free Beta (Si/Al = 4.6) with that of a templated Beta (Si/Al = 12.5) under the same hydrogen rich conditions. Strikingly, due to the lower n_{acid}/n_{Pt} ratio and the large hydrogen excess, hydrogenolysis becomes more dominant in the product distribution for Beta-12.5, resulting in a much decreased *i*-C₄ formation.

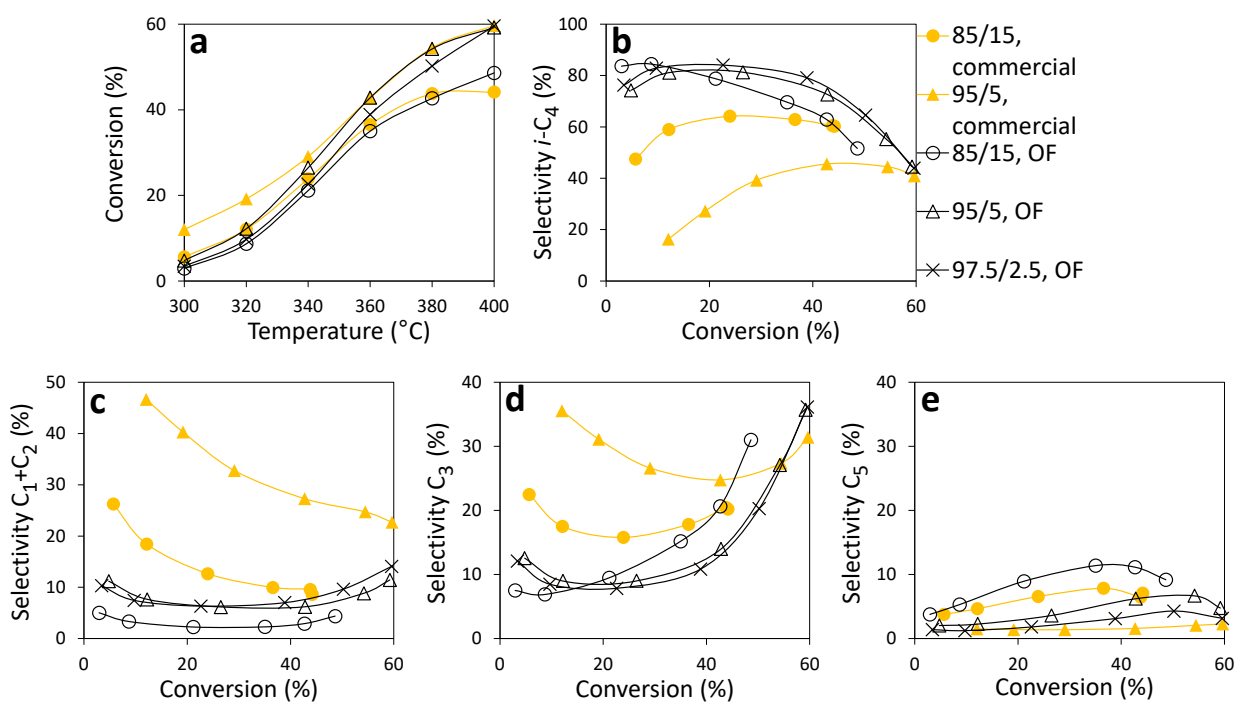


Figure 7. Effect of hydrogen partial pressure on butane isomerisation using ion-exchanged 0.1 wt% Pt on Beta-12.5 and OF-Beta-4.6. Conversion-temperature (a) and selectivity-conversion plots for *i*-C₄ (b), C₁+C₂ (c), C₃ (d), C₅ (e). Temperature, $P(H_2)/P(n-C_4)$ and WHSV were varied, total inlet flow was kept at 32.75 mL/min.

Table 7 shows the maximal *i*-C₄ yields obtained with the OSDA-free Beta at varying H₂ partial pressure, as derived from the data of Figure 7; under the most favourable conditions, yields up to 31% were reached, which is close to the thermodynamic maximum of around 35% at 360 °C (Figure S12). Because of its high acid density and the associated high isomerisation activity, the OSDA-free Beta reached its maximal *iso*-C₄ yield at lower temperatures than the commercial, templated Beta. This is of particular interest since the isomerisation is slightly exothermic, and the equilibrium is therefore more favourable at lower temperatures.

Table 7. Maximal isobutane yields derived from results obtained at different reaction temperatures. Catalyst performance as a function of H₂/*n*-C₄ is shown for an ion-exchanged 0.1wt% Pt/OF-Beta-4.6.

H ₂ / <i>n</i> -C ₄	<i>i</i> -C ₄ yield _{max.}	<i>i</i> -C ₄ selectivity	T _{max. yield} ^a (°C)
85/15	27	63	380
95/5	31	73	360
97.5/2.5	31	80	360

^a The temperature at which the highest *i*-C₄ yield and selectivity were achieved under the respective reaction conditions.

Relation between Al content of Beta zeolites and performance in C₄ isomerisation

The different performances of the templated Beta zeolite (Si/Al = 12.5) and OSDA-free Beta (Si/Al = 4.6) are striking. This raises the question whether the number of strong acid sites and the Si/Al ratio are the decisive parameters determining the performance in butane isomerisation, or whether elements specific to the zeolite formation, *e.g.* the different conditions during the templated *vs* the non-templated synthesis, play an important role. In order to elucidate this, two additional templated Beta zeolites with intermediate Si/Al ratios were acquired: first, a templated zeolite with Si/Al = 9 was commercially sourced, and secondly, an Al-rich Beta zeolite (Si/Al = 5.2) was prepared using a template, following the recipe as reported by Borade.^[43] The TPD profiles of these zeolites are included in Figure S6; the number of (strong) acid sites is similar for the samples with Si/Al = 12.5 and 9, but significantly higher for the zeolite with Si/Al = 5.2. N₂ physisorption data, X-ray patterns and electron micrographs are contained in Table 4 and Table S2, Figures S2, S3, S5, S8 and S9. While all templated Beta zeolites consist of aggregates of nanosized crystals that are smaller than 100 nm, the OSDA-free sample shows intergrown crystals of slightly larger dimensions, in the 100-300 nm range, with the discernible truncated octahedral shape that is characteristic for Beta.^[44] The samples were loaded with 0.1wt% Pt to minimise hydrogenolysis, and their catalytic data are shown in Figure 8.

The catalytic characteristics of the templated Beta-5.2 closely follow those of OF-Beta-4.6: *iso*-C₄ selectivities ~80% for conversions ~20%; nearly fully suppressed hydrogenolysis to C₁ and C₂; and equimolar formation of C₃ and C₅ at limited conversion (≤ 20%), proving that these byproducts are formed by a bimolecular mechanism. In contrast, Beta-9 is similar to Beta-12.5, with lower

iso-C₄ selectivity, more pronounced hydrogenolysis, even at 0.1 wt% of Pt, and clearly lower *iso*-C₄ yields at moderate conversions ($\leq 30\%$). Also zeolites with higher Si/Al ratios were considered, specifically OSDA-free materials that were subjected to dealumination, with Si/Al ratios of 23, 36 and 41 (Table S2, Table S4). However, these materials displayed low *iso*-C₄ selectivities and yields. Summarising, among the catalysts with *BEA topology, the Al-rich materials, either obtained *via* an OSDA-free or templated route, are superior catalysts for butane isomerisation.

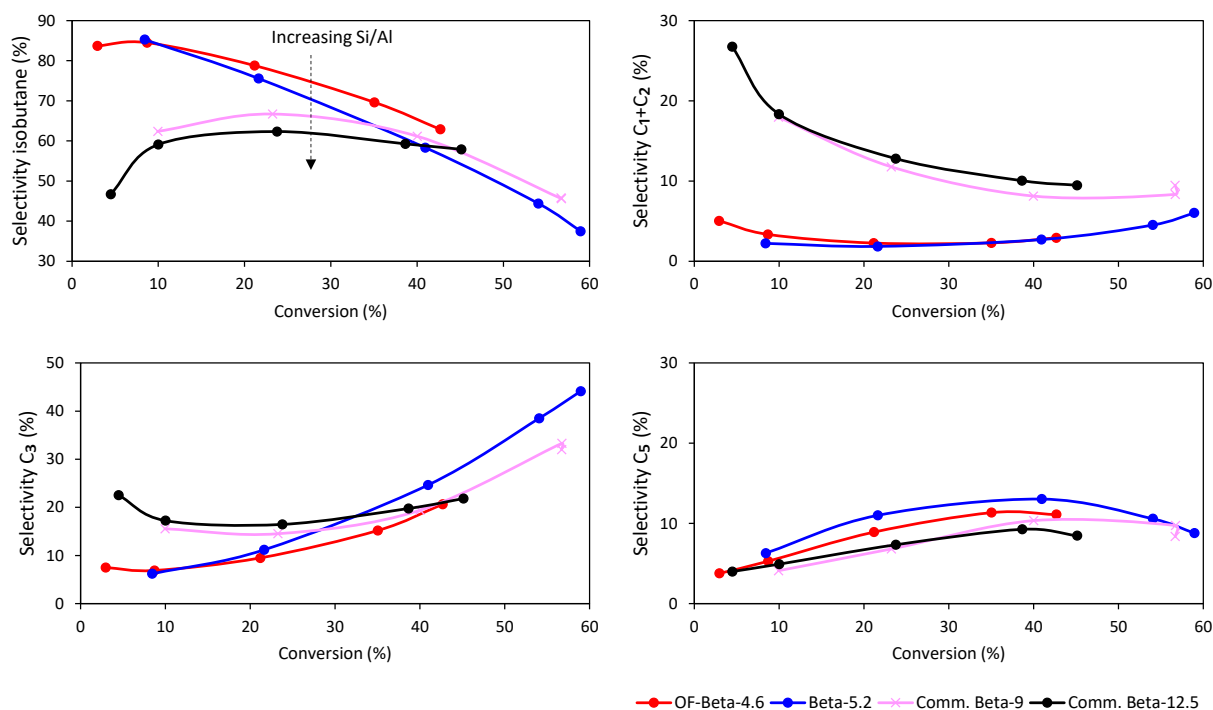


Figure 8. Selectivity-conversion plots of isobutane, C₁+C₂, C₃, and C₅ using 0.1 wt% Pt/(OF-)Beta prepared by ion exchange. Comm. = from commercial source. The number after the hyphen indicates the Si/Al ratio. Reaction conditions: P_{butane} 0.15 bar, P_{hydrogen} 0.85 bar, WHSV 3.5 h⁻¹, varied temperature.

Stability and regenerability of Pt-loaded OSDA-free Beta zeolites

A time-on-stream experiment was run using the 0.1 wt% Pt/OSDA-free Beta catalyst, with a H₂/*n*-C₄ ratio of 97.5:2.5. Hydrogen has been shown to hinder coke formation and so slow down the rate of catalyst deactivation.^[17,26,27] The plot in Figure S11 shows that after an initial decline of a few %, the conversion stayed constant for at least 15 h. Finally, we also addressed the regeneration and reuse of the catalyst (Table 8). After a first use, the 0.1 wt% Pt on OSDA-free Beta was heated under oxygen flow at 1 °C/min to 550 °C and kept for 4 h. After cooling, the catalyst was heated at 1 °C/min to 400 °C under hydrogen flow and kept again for 4 h. The *i*-C₄ yields at 360 °C from fresh and regenerated catalysts (24% and 25% respectively) were virtually identical; the same held

for the selectivities of the different products. This proves that upon appropriate treatment, the catalytic activity of the OSDA-free Beta isomerisation catalyst can be recovered completely.

Table 8. Product distribution at 41% butane conversion using 0.1wt% Pt/OF-Beta-4.6.

	<i>S</i> <i>i</i> -C ₄ (%)	<i>S</i> C ₁ +C ₂ (%)	<i>S</i> C ₃ (%)	<i>S</i> C ₅ (%)
Fresh	63	3	21	11
Regenerated	60	4	23	11

Conclusion

The results of a screening of Pt-loaded zeolites in butane isomerisation indicated that the most selective formation of isobutane in significant yields is achieved with 12-membered ring zeolites with three-dimensional pore networks. Besides the known zeolite Beta catalysts, new zeolites with YFI or MSE topologies, and with a framework Si/Al ratio of about 10, were identified as effective butane isomerisation catalysts. As an alternative to Beta zeolites prepared with organic structure directing agents, a Beta zeolite resulting from an organotemplate-free synthesis was evaluated in detail. This material, with Si/Al = 4.6, contains around twice as many strong acid sites as the standard Beta zeolite with Si/Al = 12.5. With low loadings of Pt (0.1wt%) on OSDA-free Beta, a well-balanced catalyst was obtained, which showed limited hydrogenolysis to C₁ and C₂ even in H₂-rich conditions. OSDA-free Beta reaches a maximal isobutane yield at lower temperatures than the templated Beta with Si/Al = 12.5. Isobutane selectivities near 80% could be obtained over a conversion range up to 40%. It has been explained that this high selectivity for isobutane can arise from bimolecular mechanisms, even if a contribution by monomolecular mechanisms cannot be excluded.

Overall this confirms that template-free, Al-rich zeolites like OSDA-free Beta combine economic and environmental advantages with excellent performance, at least if the catalyst and its operating conditions are well controlled to harness the activity of the large number of strong acid sites. Future developments could focus on increasing the number of strong acid sites in zeolites with MSE or YFI topologies, which this work identified as promising for bifunctional butane isomerisation.

Experimental

Platinum-loaded zeolite preparation

To prepare platinum-loaded samples with ion exchange, the target amount of tetraammineplatinum(II) chloride hydrate (Sigma-Aldrich, 98%) was first dissolved in Milli-Q water, and then added dropwise to a stirred suspension of zeolite (25 mL_{water}/g_{zeolite}). After the mixture was left stirring overnight at room temperature, the samples were washed with Milli-Q water and subsequently dried at 60 °C overnight. Samples were pelletised to sizes of 250-500 μm before calcination in oxygen at 400 °C for 4 h at a heating rate of 1 °C/min, followed by a repeat of the programme in a reductive atmosphere of hydrogen. Chloroplatinic acid hexahydrate (TCI, 37.3-38.0% Pt) was used when the Pt was incorporated using the incipient wetness impregnation

method; the target amount was dissolved in an amount of deionised water equivalent to the pore volume of the zeolite. The solution was added dropwise to the zeolite under vigorous stirring. The mixture was then left stationary overnight and subsequently dried at 60 °C. The same pelletisation/calcination/reduction procedure as detailed above was followed. The zeolites used were obtained from the following suppliers: Beta-12.5 (PQ Corporation, CP811 BL-25), Beta-9 and ferrierite (Tosoh Corporation, HSZ-920NHA and TSZ-700), ZSM-5 (Zeolyst, CBV5524G), MCM-22 (China Catalyst Holding Co., Ltd.), USY (Zeolyst, CBV720), mordenite (Chemie Uetikon, PM-1). Beta-5.2 was prepared according to the method of Borade *et al.*^[43] OF-Beta-4.6 was prepared according to Yilmaz *et al.*^[10] MCM-68 was prepared according to Otomo *et al.*^[35] YNU-5 was prepared according to Nakazawa *et al.*^[36] XRD patterns are given in Figures S1, S2 and S3. Further information is supplied in the supplementary information section (Table S1).

***n*-Butane skeletal isomerisation**

n-Butane isomerisation was performed in a fixed bed reactor at atmospheric pressure with a stainless steel tube (inner diameter 4.4 mm). In a typical test, 0.2 g of a pelletised catalyst (250-500 µm) was pre-treated in hydrogen (Air Liquide, N40) at 300 °C for 1 h prior to the reaction. A binary mixture of hydrogen and *n*-butane (Air Liquide, N25) was fed into the reactor. The H₂:*n*-C₄ ratio was kept at 5.67 and the weight hourly space velocity (WHSV) of *n*-butane was 3.5 h⁻¹. The gaseous products were analysed using an on-line gas chromatograph (Shimadzu GC-2010 Plus) equipped with a flame ionisation detector (FID) and a GsBP PLOT-Q capillary column (30 m × 0.53 mm × 30 µm). Results are reported on a molar basis.

Catalyst characterisation

Powder X-ray diffractograms were recorded on a Malvern Panalytical Empyrean diffractometer in transmission/Debye-Scherrer geometry ($1.3 < 2\theta < 45^\circ$, 0.013° step size) with a PIXcel3D detector. Ammonia temperature programmed desorption (NH₃-TPD) to determine sample acidity was measured on a Quantachrome ChemBET PULSAR. The sample (200 mg) was dried overnight in a muffle furnace, then heated to 600 °C in helium (20 mL/min) at the instrument. The sample was subsequently dosed with ammonia (Air Liquide, N38) at 25 °C and physisorbed ammonia was removed at 50 °C in helium. Afterwards, TCD signals of the desorbed ammonia were recorded while heating the sample in helium to 600 °C at 10 °C/min. Quantification of sample acidity was performed using a calibration of 75 µL ammonia pulse. The NH₃-TPD profile was fitted using three peaks to obtain the distribution of acid strength; the strong acid site density was thus determined based on the integrated area under the high-temperature peak. For metal dispersion determinations, CO chemisorption experiments were performed on a Quantachrome ChemBET PULSAR. The sample was first dried overnight in an oven. In the apparatus, the sample is reduced in hydrogen at 200 °C, then the sample is pulsed with CO (Air Liquide, N37) and flushed with He alternately at 25 °C. Analysis was done under the assumption of a stoichiometry of 1 CO molecule per surface Pt atom. Nitrogen physisorption isotherms to determine textural properties of the samples were collected at -196 °C on a Micromeritics 3Flex surface analyzer. Samples were degassed at 200 °C for 12 h under vacuum before data collection. The specific surface areas were obtained by the BET method, the micropore area, external area, and micropore volume were estimated from t-plot method, and the mesopore volume was estimated by DFT method. High-

angle annular dark-field scanning transmission electron microscopy (HAADF-STEM) was used to image selected samples.

Acknowledgements

This work was supported by BASF SE under the INCOE framework (International Network of Centers of Excellence). Sam Van Minnebruggen thanks FWO Flanders for a doctoral fellowship. The authors thank Dr. Jannick Vercammen (KU Leuven) for his help in the Beta-5.2 synthesis, and Dr. Philipp Müller (BASF SE) for the TEM measurements.

Keywords

Al-rich zeolites, bifunctional catalysts, isobutane, isomerization, OSDA-free Beta

References

- [1] G. Alfke, W. W. Irion, O. S. Neuwirth, in *Ullmann's Encycl. Ind. Chem.*, **2012**, pp. 207–262.
- [2] M. Winterberg, E. Schulte-Körne, U. Peters, F. Nierlich, in *Ullmann's Encycl. Ind. Chem.*, **2012**, pp. 119–130.
- [3] S. T. Sie, in *Handb. Heterog. Catal.* (Eds.: G. Ertl, H. Knözinger, F. Schüth, J. Weitkamp), **2008**, pp. 2809–2830.
- [4] E. Garbowski, J. P. Candy, M. Primet, *J. Chem. Soc. Faraday Trans. 1 Phys. Chem. Condens. Phases* **1983**, *79*, 835–844.
- [5] A. C. Oliveira, N. Essayem, A. Tuel, J. M. Clacens, Y. Ben Tâarit, *J. Mol. Catal. A Chem.* **2008**, *293*, 31–38.
- [6] P. Wang, W. Zhang, Q. Zhang, Z. Xu, C. Yang, C. Li, *Appl. Catal. A Gen.* **2018**, *550*, 98–104.
- [7] P. Cañizares, A. De Lucas, F. Dorado, *Appl. Catal. A Gen.* **2000**, *196*, 225–231.
- [8] P. Cañizares, F. Dorado, P. Sánchez-Herrera, *Appl. Catal. A Gen.* **2001**, *217*, 69–78.
- [9] F. Dorado, R. Romero, P. Cañizares, *Appl. Catal. A Gen.* **2002**, *236*, 235–243.
- [10] B. Yilmaz, U. Müller, M. Feyen, S. Maurer, H. Zhang, X. Meng, F. S. Xiao, X. Bao, W. Zhang, H. Imai, T. Yokoi, T. Tatsumi, H. Gies, T. De Baerdemaeker, D. De Vos, *Catal. Sci. Technol.* **2013**, *3*, 2580–2586.
- [11] A. Corma, M. I. Juan-Rajadell, J. M. López-Nieto, A. Martinez, C. Martínez, *Appl. Catal. A, Gen.* **1994**, *111*, 175–189.
- [12] T. De Baerdemaeker, B. Yilmaz, U. Müller, M. Feyen, F. S. Xiao, W. Zhang, T. Tatsumi, H. Gies, X. Bao, D. De Vos, *J. Catal.* **2013**, *308*, 73–81.
- [13] S. Van Minnebruggen, T. De Baerdemaeker, K. Y. Cheung, A. N. Parvulescu, U. Müller, P. Tomkins, R. de Oliveira-Silva, X. Meng, F. S. Xiao, T. Yokoi, W. Zhang, D. Sakellariou, D. De Vos, *J. Catal.* **2022**, *406*, 206–212.
- [14] W. Zhang, P. Wang, C. Yang, C. Li, *Catal. Letters* **2019**, *149*, 1017–1025.
- [15] R. A. Asuquo, G. Eder-Mirth, J. A. Lercher, *J. Catal.* **1995**, *155*, 376–382.
- [16] J. E. Samad, J. Blanchard, C. Sayag, C. Louis, J. R. Regalbuto, *J. Catal.* **2016**, *342*, 203–212.
- [17] R. A. Asuquo, G. Eder-Mirth, K. Seshan, J. A. Z. Pieterse, J. A. Lercher, *J. Catal.* **1997**, *168*, 292–300.
- [18] E. Baburek, J. Nováková, *Appl. Catal. A Gen.* **2000**, *190*, 241–251.
- [19] H. Liu, V. Adeeva, G. D. Lei, W. M. H. Sachtler, *J. Mol. Catal. A Chem.* **1995**, *100*, 35–48.

- [20] P. Wang, S. Wang, Y. Yue, H. Zhu, T. Wang, X. Bao, *Microporous Mesoporous Mater.* **2020**, *309*, 110547.
- [21] F. Rodríguez-Reinoso, I. Rodríguez-Ramos, C. Moreno-Castilla, A. Guerrero-Ruiz, J. D. López-González, *J. Catal.* **1987**, *107*, 1–7.
- [22] K. J. Chao, H. C. Wu, L. J. Leu, *J. Catal.* **1995**, *157*, 289–293.
- [23] K. Na, T. Okuhara, M. Misono, *J. Catal.* **1997**, *170*, 96–107.
- [24] S. De Rossi, G. Moretti, G. Ferraris, D. Gazzoli, *Catal. Letters* **2002**, *78*, 119–123.
- [25] V. Adeeva, W. M. H. Sachtler, *Appl. Catal. A Gen.* **1997**, *163*, 237–243.
- [26] J. C. Yori, J. C. Luy, J. M. Parera, *Catal. Today* **1989**, *5*, 493–502.
- [27] J. C. Yori, J. C. Luy, J. M. Parera, *Appl. Catal.* **1989**, *46*, 103–112.
- [28] T. Kurniawan, O. Muraza, I. A. Bakare, M. A. Sanhoob, A. M. Al-Amer, *Ind. Eng. Chem. Res.* **2018**, *57*, 1894–1902.
- [29] M. T. Tran, N. S. Gnep, G. Szabo, M. Guisnet, *J. Catal.* **1998**, *174*, 185–190.
- [30] J. I. Villegas, N. Kumar, T. Salmi, D. Y. Murzin, T. Heikkilä, P. Hudec, A. Smiešková, *Stud. Surf. Sci. Catal.* **2005**, *158*, 1859–1866.
- [31] M. J. Wulfers, F. C. Jentoft, *J. Catal.* **2015**, *330*, 507–519.
- [32] A. Feller, J. A. Lercher, *Adv. Catal.* **2004**, *48*, 229–295.
- [33] G. S. Nivarthi, Y. He, K. Seshan, J. A. Lercher, *J. Catal.* **1998**, *176*, 192–203.
- [34] P. A. Jacobs, J. A. Martens, *Stud. Surf. Sci. Catal.* **1991**, *58*, 445–496.
- [35] R. Otomo, T. Nishitoba, R. Osuga, Y. Kunitake, Y. Kamiya, T. Tatsumi, T. Yokoi, *J. Phys. Chem. C* **2018**, *122*, 1180–1191.
- [36] N. Nakazawa, T. Ikeda, N. Hiyoshi, Y. Yoshida, Q. Han, S. Inagaki, Y. Kubota, *J. Am. Chem. Soc.* **2017**, *139*, 7989–7997.
- [37] M. A. Coelho, D. E. Resasco, E. C. Sikabwe, R. L. White, *Catal. Letters* **1995**, *32*, 253–262.
- [38] J. I. Villegas, N. Kumar, T. Heikkilä, V. Lehto, T. Salmi, D. Y. Murzin, *Chem. Eng. J.* **2006**, *120*, 83–89.
- [39] E. Baburek, J. Nováková, *Appl. Catal. A Gen.* **1999**, *185*, 123–130.
- [40] B. Xie, H. Zhang, C. Yang, S. Liu, L. Ren, L. Zhang, X. Meng, B. Yilmaz, U. Müller, F. S. Xiao, *Chem. Commun.* **2011**, *47*, 3945–3947.
- [41] J. I. Villegas, N. Kumar, T. Heikkilä, A. Smiešková, P. Hudec, T. Salmi, D. Y. Murzin, *Appl. Catal. A Gen.* **2005**, *284*, 223–230.
- [42] Y. Liu, M. Misono, *Materials (Basel)*. **2009**, *2*, 2319–2336.

- [43] R. B. Borade, A. Clearfield, *Microporous Mater.* **1996**, 5, 289–297.
- [44] G. Majano, L. Delmotte, V. Valtchev, S. Mintova, **2009**, 4184–4191.

Graphical abstract



A bifunctional catalyst using a low Pt content and Al-rich zeolite Beta from seeded synthesis showed efficient catalytic activity in the isomerisation of butane to give good isobutane yields.